Fish and Shellfish Immunology 87 (2019) 534–545

Contents lists available at ScienceDirect

Fish and Shellfish Immunology

journal homepage: www.elsevier.com/locate/fsi

Full length article

Proteomic and metabolomic responses in hepatopancreas of whiteleg shrimp *Litopenaeus vannamei* infected by microsporidian *Enterocytozoon hepatopenaei*

Mingxiao Ning[a], Panpan Wei[a], Hui Shen[d], Xihe Wan[d], Mingjian Jin[f], Xiangqian Li[b], Hao Shi[b], Yi Qiao[d], Ge Jiang[d], Wei Gu[c,g], Wen Wang[a], Li Wang[e,**], Qingguo Meng[c,g,*]

[a] College of Life Sciences, Nanjing Normal University, 1 Wenyuan Road, Nanjing, 210023, China
[b] Jiangsu Provincial Key Construction Laboratory of Probiotics Preparation, Huaiyin Institute of Technology, Huaian, 223003, China
[c] Jiangsu Key Laboratory for Aquatic Crustacean Diseases, College of Marine Science and Engineering, Nanjing Normal University, 1 Wenyuan Road, Nanjing, 210023, China
[d] Institute of Oceanology and Marine Fisheries, Jiangsu, Jiangsu, 226007, China
[e] College of Life Science and Technology, Southwest Minzu University, Chengdu, 610041, China
[f] Rudong Center for Control and Prevention of Aquatic Animal Infectious Disease, 25# Changjiang Road, Rudong, 226400, China
[g] Co-Innovation Center for Marine Bio-Industry Technology of Jiangsu Province, Lianyungang, Jiangsu, 222005, China

ARTICLE INFO

Keywords:
Enterocytozoon hepatopenaei
Litopenaeus vannamei
Hepatopancreatic microsporidiosis
Proteomics
Metabolomics

ABSTRACT

Enterocytozoon hepatopenaei (EHP) causes hepatopancreatic microsporidiosis (HPM) in shrimp. HPM is not normally associated with shrimp mortality, but is associated with significant growth retardation. In this study, the responses induced by EHP were investigated in hepatopancreas of shrimp *Litopenaeus vannamei* using proteomics and metabolomics. Among differential proteins identified, several (e.g., peritrophin-44-like protein, alpha2 macroglobulin isoform 2, prophenoloxidase-activating enzymes, ferritin, Rab11A and cathepsin C) were related to pathogen infection and host immunity. Other proteomic biomarkers (i.e., farnesoic acid *o*-methyltransferase, juvenile hormone esterase-like carboxylesterase 1 and ecdysteroid-regulated protein) resulted in a growth hormone disorder that prevented the shrimp from molting. Both proteomic KEGG pathway (e.g., "Glycolysis/gluconeogenesis" and "Glyoxylate and dicarboxylate metabolism") and metabolomic KEGG pathway (e.g., "Galactose metabolism" and "Biosynthesis of unsaturated fatty acids") data indicated that energy metabolism pathway was down-regulated in the hepatopancreas when infected by EHP. More importantly, the changes of hormone regulation and energy metabolism could provide much-needed insight into the underlying mechanisms of stunted growth in shrimp after EHP infection. Altogether, this study demonstrated that proteomics and metabolomics could provide an insightful view into the effects of microsporidial infection in the shrimp *L. vannamei*.

1. Introduction

Microsporidia are small obligate intracellular parasites and recently reclassified with the fungi and not to be protists [1,2]. Almost half of the reported genera of microsporidia infect aquatic hosts, and usually has chronic and sublethal effects on hosts [3,4]. However, microsporidia pathogenesis are vastly under-reported in aquatic systems. Hepatopancreatic microsporidiosis (HPM), one of the serious epidemics in *Litopenaeus vannamei*, is caused by *Enterocytozoon hepatopenaei* (EHP) and is currently dramatically increasing the economic losses in the shrimp harvest in Southeast Asia [5–7]. EHP was reported for the first time in pond-reared *Penaeus monodon* in Thailand [8] and later in Vietnam, China, Indonesia, Malaysia and India [5,9]. As other microsporidia, the sign of stunted growth was observed in EHP-infected shrimp. Further research revealed that EHP mainly infect epithelial cells of the hepatopancreas of wild and farmed decapod crustaceans [8]. In addition, the research of microsporidian intensively focused on the pathogen aspects including the molecular phylogenetic analysis, development of novel detection assays, histopathology and comparative genome research [6,7,10]. However, limited information was available about the host responses, which could provide important information to elucidate the diverse aspects of the host-pathogen interactions.

* Corresponding author. Jiangsu Key Laboratory for Aquatic Crustacean Diseases, College of Marine Science and Engineering, Nanjing Normal University, 1 Wenyuan Road, Nanjing, 210023, China.
** Corresponding author.
E-mail addresses: 371094841@qq.com (L. Wang), mlzzcld@aliyun.com (Q. Meng).

https://doi.org/10.1016/j.fsi.2019.01.051
Received 20 November 2018; Received in revised form 25 January 2019; Accepted 30 January 2019
Available online 02 February 2019

It is well known that host's immune response can be activated when pathogenic microorganism invading host. Invertebrate innate immune response plays a dominant role in protecting hosts from invading pathogens because of lack of adaptive immunity [11]. The innate defense system of invertebrates is composed of cellular and humoral immunity response mechanisms that include enzymes and proteins in the prophenoloxidase (proPO) activation and blood coagulation systems [12]. So EHP may cause the activation of proPO or other immune system in *L. vannamei*. In addition, as obligate intracellular parasites, microsporidians are highly dependent on their hosts, and have an expanded repertoire of transport proteins to exploit the rich environment in the host cell cytoplasm [10]. This feature suggests that microsporidia have a potential to change host nutritional and metabolic pathways. How EHP parasitization produces the metabolic stresses in the shrimp *L. vannamei* is still unknown. To study the change of host immune response and metabolic pathway, many traditional approaches have been applied [13–15]. However, these researches obviously presented a primary understanding of responses of *L. vannamei* to EHP challenges.

With the emergence and development of systems biology techniques, including genomics, transcriptomics, proteomics and metabolomics, new opportunities are offered with great potential in unraveling biological problems, and have been successfully employed in multiple areas such as environmental sciences, toxicological effects and immunology [16–18]. Among these approaches, proteomics is a means of comprehensive interpretation, which can be used to describe more direct molecular responses than conventional transcriptomic or genomics [19]. As a kind of highly sensitive proteomic platform, the isobaric label tandem mass tags (TMT) was used to identify differential proteome frequently [20,21]. So far, many studies have reported about using proteomic techniques to study the response of invertebrates against various pathogenic microorganisms [14,19,20]. In addition, metabolomics usually focuses on the whole set of low molecular weight (< 1000 Da) metabolites. The metabolites represent the collection of all metabolites in organs, tissues, biofluids, or even whole organisms, which are the end products of various biological systems [22]. A comparative analysis of metabolomes can give significant evidence in interpreting metabolite perturbations in response to exogenous factors affecting metabolism of organisms as well as proteomics [23,24]. These perturbed metabolites and proteins are a definite set of molecular biomarkers related to biological effects of stressors [17,18]. Therefore, a combination of proteomics and metabolomics can yield a better understanding of the biological responses that an organism makes to environmental stressors [25]. To date, no attempt has been made to test the responses induced by EHP in *L. vannamei* using a combined proteomic and metabolomic approach.

In this study, EHP infection in *L. vannamei* with stunted growth was confirmed using PCR assay firstly. Secondly, the proteomic and metabolomic profiling were applied to show a global survey of differentially identified proteins and metabolites between EHP-infected and healthy shrimp. Thirdly, the patterns of some differential proteins were further assessed by qRT-PCR in EHP natural infections. It was found that not only the innate immune system of *L. vannamei* was activated, but also the growth hormone and energy metabolism of *L. vannamei* were disturbed by EHP though these studies. These results could help us to better understand the immune relationship between *L. vannamei* and EHP and molecular mechanisms of stunted growth of shrimps in EHP infection.

2. Materials and methods

2.1. PCR assay for detecting EHP from shrimp samples

L. vannamei were obtained from commercial shrimp ponds in Nantong, Jiangsu Province, China. DNA extractions of hepatopancreas from healthy shrimps and slow-growing shrimps infected by EHP were prepared with the EasyPure Genomic DNA Kit (Transgen, China). Templates were tested further for concentration and purity with a spectrophotometer (Thermo, USA). The primers for detecting the EHP are EHP-510F and EHP-510R (Table S1). The PCR amplification was carried out in a 25-μL reaction mixture, which contained 12.5 μL PrimeSTAR Max Premix (Takara, Japan), 0.2 μM of each primer and 1 μL of extracted DNA (100 ng μl^{-1}). The amplification was performed with the following cycling parameters: initial denaturation at 98 °C for 3 min, followed by 35 cycles of 98 °C for 5 s, 55 °C for 15 s, and 72 °C for 10 s, and a final extension at 72 °C for 10 min. Following PCR, PCR products were analyzed in a 1.2% agarose gel containing ethidium bromide. The amplified DNA was visualized under UV illumination using a gel documentation system (Bio-rad, USA) and sequenced by the Springen Biotechnology Company in Nanjing. Meanwhile, *Vibrio* spp. infection in the shrimps was tested using the primers rpoA-F and rpoA-R (Table S1) for PCR assay [26]. The shrimps without *vibrio* infection were used for the omics study. The copy number of EHP was examined by absolute real-time PCR [27] from every shrimp using the primers EHP-185-qF and EHP-185-qR (Table S1). Absolute real-time PCR analyses were performed in triplicate.

2.2. Protein extraction and digestion

The hepatopancreas samples were collected from five healthy and EHP-infected shrimps, respectively. After collection, the samples were sonicated three times on ice using a high intensity ultrasonic processor (Scientz, China) in lysis buffer (8 M urea, 2 mM EDTA, 10 mM DL-Dithiothreitol (DTT) and 1% Protease Inhibitor Cocktail). The remaining debris was removed by centrifugation at 20,000 × *g* at 4 °C for 10 min. The protein was precipitated with cold 15% trichloroacetic acid (TCA) for 4 h at −20 °C. And then, the remaining precipitate was washed with cold acetone for three times. The protein was re-dissolved in buffer (8 M urea, 100 mM triethyl ammonium bicarbonate (TEAB), pH 8.0) and the protein concentration in the supernatant was determined with 2-D Quant kit (GE Healthcare) according to the manufacturer's instructions. The protein solution was treated with 5 mM DTT for 30 min at 56 °C and alkylated with 11 mM iodoacetamide (IAA) for 15 min at room temperature in darkness. For trypsin digestion, the protein sample was diluted by adding 200 mM triethylamine borane (TEAB) to urea concentration less than 2 M. Finally, trypsin was added at 1:50 trypsin-to-protein mass ratio for the first digestion overnight and 1:100 trypsin-to-protein mass ratio for a second 4-h digestion. Approximately 100 μg protein for each sample was digested with trypsin for the following experiments.

2.3. Metabolite extraction

30 mg of accurately weighed hepatopancreas samples were transferred to an Eppendorf tube from six healthy and EHP-infected shrimps, respectively. Two small steel balls were added to the tube. 20 μL internal standard (2-chloro-L-phenylalanine in methanol, 0.3 mg mL^{-1}) and 600 μL extraction solvent with methanol/water (4/1, v/v) were added to each sample. Samples were stored at −80 °C for 2 min and then ground at 60 HZ for 2 min. 120 μL of chloroform was added to the samples, then the samples were vigorously vortexed and followed by 10 min ultrasound-associated extraction at ambient temperature, then stored at 4 °C for 10 min. The samples were centrifuged at 12,000 rpm for 10 min at 4 °C. An aliquot of the 400-μL supernatant was transferred to a glass-sampling vial for vacuum drying at room temperature. And 80 μL of methoxylamine hydrochloride (dissolved in pyridine, 15 mg mL^{-1}) was subsequently added. The resultant mixture was vortexed vigorously for 2 min and incubated at 37 °C for 90 min. 80 μL of N, *O*-bis (trimethylsilyl) trifluoroacetamide (with 1% trimethylchlorosilane) and 20 μL *n*-hexane were added into the mixture, which was vortexed vigorously for 2 min and then derivatized at 70 °C for 60 min. The samples were placed at ambient temperature for 30 min before gas chromatography-mass spectrometry (GC/MS) analysis.

2.4. TMT labeling and high performance liquid chromatography (HPLC) fractionation

After protein digestion, peptides were desalted using Strata X C18 SPE column (Phenomenex, USA) and dried with a vacuum concentration meter. The dried peptide powder was reconstituted in 1M TEAB and further processed according to the manufacturer's protocol of 6-plex TMT kit. The sample was then separated into fractions by high pH reverse-phase HPLC using an Agilent 300 Extend C18 column (5-μm particles, 4.6 mm ID, 250 mm length). Briefly, peptides were first separated with a gradient of 2%–60% acetonitrile in 10 mM ammonium bicarbonate (pH 9.0) during 80 min yielding 80 fractions. Then, the peptides were combined into 18 fractions and dried by vacuum centrifuging.

2.5. Liquid chromatography-mass spectrometry (LC-MS/MS) analyses

Peptides were dissolved in 0.1% formic acid (FA), and directly loaded onto a reversed-phase pre-column (Acclaim PepMap 100, Thermo, USA). Peptide separation was performed using a reversed-phase analytical column (Acclaim PepMap RSLC, Thermo, USA). The gradient was comprised of an increase from 6% to 22% solvent B (0.1% FA in 98% acetonitrile (ACN)) during 26 min, then raised further to 22%–35% in 8 min, culminating at 80% in 3 min and then held at 80% for the last 3 min; all at a constant flow rate of 400 nL/min on an EASY-nLC 1000 Ultra Performance Liquid Chromatography (UPLC) system. The peptides were loaded onto an NSI source followed by tandem mass spectrometry (MS/MS) in Q Exactive Plus™ (Thermo, USA) coupled online to the UPLC. Intact peptides were detected in the Orbitrap at a resolution of 70,000. Peptides were selected for MS/MS using NCE setting as 28; ion fragments were detected in the Orbitrap at a resolution of 17,500. A data-dependent procedure that alternated between one MS scan followed by 20 MS/MS scans was applied for the top 20 precursor ions above a threshold ion count of 1E4 in the MS survey scan with 30.0 s dynamic exclusion. The electrospray voltage applied was 2.0 kV. Automatic gain control (AGC) was used to prevent overfilling of the Orbitrap; 5E4 ions were accumulated for generation of MS/MS spectra. For MS scans, the *m/z* scan range was 350–1800. Fixed first mass was set as 100 *m/z*.

2.6. Gas chromatography-mass spectrometry (GC/MS) analysis

The derivatized samples were analyzed on an Agilent 7890B gas chromatography system coupled to an Agilent 5977A MSD system (Agilent Technologies Inc., CA, USA). A DB-5MS fused-silica capillary column (30 m × 0.25 mm × 0.25 μm, Agilent J & W Scientific, Folsom, CA, USA) was utilized to separate the derivatives. Helium (> 99.999%) was used as the carrier gas at a constant flow rate of 1 mL/min through the column. The injector temperature was maintained at 260 °C. Injection volume was 1 μL by splitless mode. The initial oven temperature was 60 °C, and subsequently ramped up to 125 °C at a rate of 8 °C/min, then up to 210 °C at a rate of 5 °C/min, further up to 270 °C at a rate of 10 °C/min, additionally to 305 °C at a rate of 20 °C/min, and finally held at 305 °C for 5 min. The temperature of MS quadrupole and ion source (electron impact) was set to 150 and 230 °C, respectively. The collision energy was 70 eV. Mass spectrometric data was acquired in a full-scan mode (*m/z* 50–500), and the solvent delay time was set to 5 min.

2.7. Data analysis

Proteomics Data. The resulting MS/MS data was processed using MaxQuant with integrated Andromeda search engine (v.1.5.2.8). Tandem mass spectra were identified by *L. vannamei* SwissProt database using the proteins sequences predicted by transcriptome database (Tables S2, 3417 proteins, unpublished data). Trypsin/P was used as the cleavage enzyme allowing up to 2 missing cleavages. Mass error was set to 10 peptide mass error parts per million for precursor ions and 0.02 Da for fragment ions. Carbamidomethyl on cysteine, were specified as fixed modification, and oxidation on methionine and acetylation on protein N-term was specified as variable modifications. For the protein quantification method, TMT 6-plex was selected in Mascot (Matrix Science, UK). False discovery (FDR) rate was adjusted to < 1% at the protein, peptide and propensity score matching level. And each confident protein identification involved at least one unique peptide. The quantitative protein ratios were weighted and normalized by the median ratio in Mascot. We only used ratios with $p < 0.05$, and only changes of > 2-fold were considered as significant. Functional annotations of the proteins were conducted using Blast2GO program against the non-redundant protein database (NR; NCBI).

Metabonomics Data. ChemStation (version E.02.02.1431, Agilent, USA) was used to convert the file format (D) of raw data from the apparatus to common data format (CDF). ChromaTOF (version 4.34, LECO, St Joseph, MI) was used to analyze the data. Metabolites were qualitatively identified by NIST and Fiehn database. After alignment with Statistic Compare component, the 'raw data array' (.cvs) was obtained from raw data with three dimension data sets including sample information, peak names, retention time-*m/z* and peak intensities. In the 'data array', all internal standards and any known pseudo positive peaks (caused by background noise, column bleed or BSTFA derivatization procedure) were removed. The data was normalized to total peak area of each sample, and multiplied by 10,000. Meanwhile, the peaks from the same metabolite were de-redundant and integrated.

Orthogonal Partial least-squares-discriminant analyses OPLS-DA were performed to visualize the metabolic difference among experimental groups, after mean centering and unit variance scaling. The Hotelling's T2 region, shown as an ellipse in score plots of the models, defines the 95% confidence interval of the modeled variation. Variable importance in the projection (VIP) ranks the overall contribution of each variable to the OPLS-DA model, and those variables with VIP > 1 are considered relevant for group discrimination.

In this study, the default 7-round cross-validation was applied with one-seventh of the samples being excluded from the mathematical model in each round, in order to guard against overfitting. The differential metabolites were selected on the basis of the combination of a statistically significant threshold of VIP values obtained from the OPLS-DA model and *p*-values from a two-tailed Student's t-test on the normalized peak areas, where metabolites with VIP > 1 and $p < 0.05$ were included, respectively.

2.8. Pathway analysis

Firstly, a KEGG database description of annotated protein was obtained using Kyoto Encyclopedia of Genes and Genomes (KEGG) online service tools KAAS. Meanwhile, a differential metabolites KEGG ID number was obtained using the identification (ID) transformation function of MBRole website (http://csbg.cnb.csic.es/mbrole/). The mapping of the annotation result on the KEGG pathway database was obtained using KEGG online service tools KEGG mapper (http://www.genome.jp/kegg/mapper.html). To test the enrichment of the differential proteins and metabolites against all identified proteins and metabolites, the pathway enrichment statistics were performed by a two-tailed Fisher's exact test. Correction for multiple hypothesis testing was carried out using standard false discovery rate control methods. The pathway with a corrected significance level of $p < 0.05$ was considered significant. There is no taxonomic restriction for the pathway analysis.

2.9. Quantitative real-time (qRT-PCR) analysis

The hepatopancreases were dissected-out and collected from five healthy and EHP-infected shrimps, respectively. After extraction, total RNA was reverse-transcribed into cDNA with a PrimeScript RT reagent

Kit (Takara, Japan). 18S rRNA was used as a housekeeping gene. QRT-PCR was carried out with a StepOnePlus™ Real-Time PCR System (Applied Biosystems, USA) to study the expression of immune and growth related genes in the hepatopancreas. The PCR reaction was performed in a 10-μL volume, with a SYBR Premix Ex Taq™ Kit (Takara, Japan), 0.4 μM of each specific primer (Table S1) and 1 μL of cDNA in StepOnePlus™ Real-Time PCR System using the following procedure: initial denaturation at 95 °C for 30s; followed by 40 cycles of amplification (95 °C for 10 s, 60 °C for 45 s, and 72 °C for 30 s). The amplifications were performed in a 96-well plate, and each sample had three replicates. Then, a melting curve of the amplicon was examined to determine amplification specificity. Statistical analysis was performed using SPSS software (Ver11.0). Data represent the mean ± standard error (S.E.). Statistical significance was determined by Student's *t*-test. Significance was set at $p < 0.05$.

3. Results

3.1. The detection of EHP infection in shrimp

There was no specific clinical sign associated with EHP-infected shrimp, except stunted growth without distinctly increased mortality. The size of the stunted shrimp was nearly half the size of non-infected shrimp at a particular age (Fig. S1). The primers EHP-510F/R of the 18S rRNA gene [9] from the EHP genome were selected to carry out PCR using DNA extracted from stunted growth and healthy shrimps. As shown in Fig. 1A, the PCR results revealed the appearance of an obvious band at the expected size of 510 bp for the presence of EHP [28]. Absolute real-time PCR [27] results showed that the copy numbers of EHP were 8072/ng, 3168/ng, 2500/ng and 5133/ng total DNA, respectively (Fig. 1B). These data suggested that there are large numbers of EHP in stunted growth shrimps, but not in healthy shrimps.

3.2. Protein profiling

All MS/MS spectrums were processed using MaxQuant software. As shown in (Fig. S2), TMT label-based quantitative analysis of *L. vannamei* hepatopancreas proteome showed that 3417 protein groups were identified, among which 2862 proteins were quantified. The basic information of identified proteins is presented in Table S3. Gene ontology (GO) analysis of differential proteins in hepatopancreas was based on biological process (Fig. 2A), cellular component (Fig. 2B) and molecular function (Fig. 2C). Differential proteins were identified using GO for gene function classification in the hepatopancreas. Among the biological process category, “metabolic process” (42%) was the most commonly represented, followed by “cellular process” (22%) and “single-organism process” (18%) (Fig. 2A). Proteins involved in the “cell” (33%), “macromolecular complex” (24%) and “organelle” (23%) groups were notably represented in the cellular components category (Fig. 2B). In the category of molecular function, a significant proportion of clusters were assigned to “catalytic activity” (41%) and 39% to “binding” (Fig. 2C). These data further suggested that shrimp metabolic process and enzyme activity changed significantly after microsporidium infection.

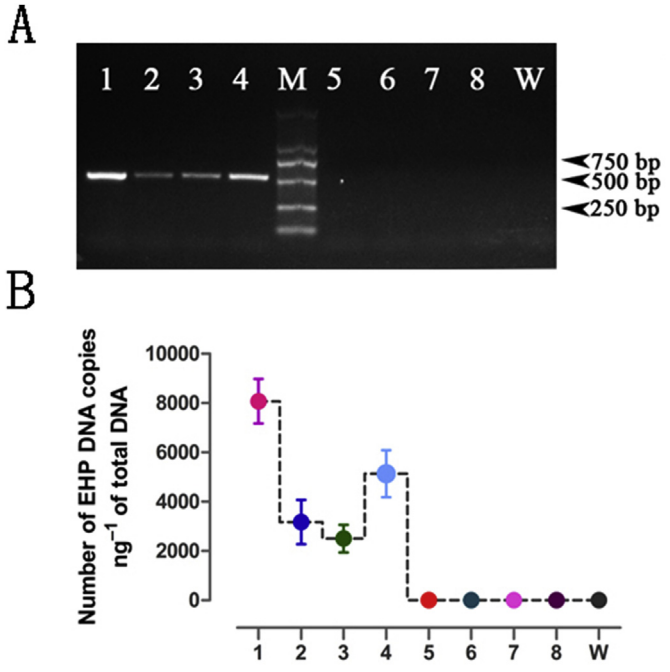

Fig. 1. PCR assay (A) and absolute real-time PCR (B) for detection of microsporidia in stunted growth and healthy shrimp. PCR amplification product (~510 bp) obtained using EHP-specific primers. 1–4, positive samples; 5–8, negative samples; M, marker; W, water.

3.3. TMT label-based quantification

Using a 2-fold increase or decrease in protein abundance as a benchmark for physiologically significant change, a total of 266 differential proteins were reliably quantified by TMT label-based quantitative analysis. 148 up-regulated and 118 down-regulated proteins were identified subsequent to EHP infection. Of the up-regulated proteins, 24, 6, 7, 57, 16, 26 and 12 proteins were involved with immunologic proteins, growth associated proteins, calcium related proteins, physiologic proteins, cytoskeleton/extracellular proteins, intracellular proteins and unknown/hypothetical proteins, respectively. The up-regulated immunologic proteins included alpha2 macroglobulin isoform 2 (α2M), peritrophin-44-like (P44L) protein, prophenoloxidase activating enzyme (PPAE) and lysozyme with 2.3-fold, 14.0-fold, 2.6-fold, 3.1-fold change, respectively (Table 1). In addition, it also included beta-1, 3-gluca binding protein (BGBP), C-type lectin, serine proteinase inhibitor, etc. The up-regulated growth associated proteins included ecdysteroid-regulated protein (ERP) with 7.0-fold change and chitin binding-like protein with 2.9-fold change (Table 1). And, farnesoic acid *O*-methyltransferase (FaMeT), juvenile hormone esterase-like protein (JHEP), myosin heavy chain type 2 and myosin light chain belong to up-regulated proteins (Table 1). The up-regulated proteins identified with notable physiologic roles and the corresponding TMT label-based quantitative ratios are presented in Table S4.

Of the down-regulated proteins, 9, 6, 3, 80, 4, 6 and 10 proteins were involved within the immune system proteins, growth associated proteins, calcium related proteins, physiologic processes proteins, cytoskeleton/extracellular proteins, intracellular protein and unknown/hypothetical proteins, respectively. The down-regulated immunologic proteins included cathepsin C (CatC), ferritin and Rab11A with 0.2-fold, 0.3-fold and 0.5-fold change, respectively (Table 1). In addition, it also included cathepsin l, C-type lectin, etc. Juvenile hormone esterase-like carboxylesterase 1 (JHEC1) with 0.5-fold change, chitinase 1C and steroid reductase belong to down-regulated growth associated proteins (Table 1). The down-regulated proteins identified with known physiologic functions and the corresponding TMT label-based quantitative ratios are presented in Table S5.

3.4. Metabolomic responses in hepatopancreas of L. vannamei challenged by EHP

There were 1138 peaks detected from all samples and quality controls. The total detectable metabolites were 423. The data was performed with PLS-DA analysis to discriminate the metabolic profiles between healthy and EHP-infected groups. As shown in Fig. 3A, PLS-DA of metabolites showed a significant difference between EHP-infected and healthy groups. Then, a supervised statistical method OPLS-DA was

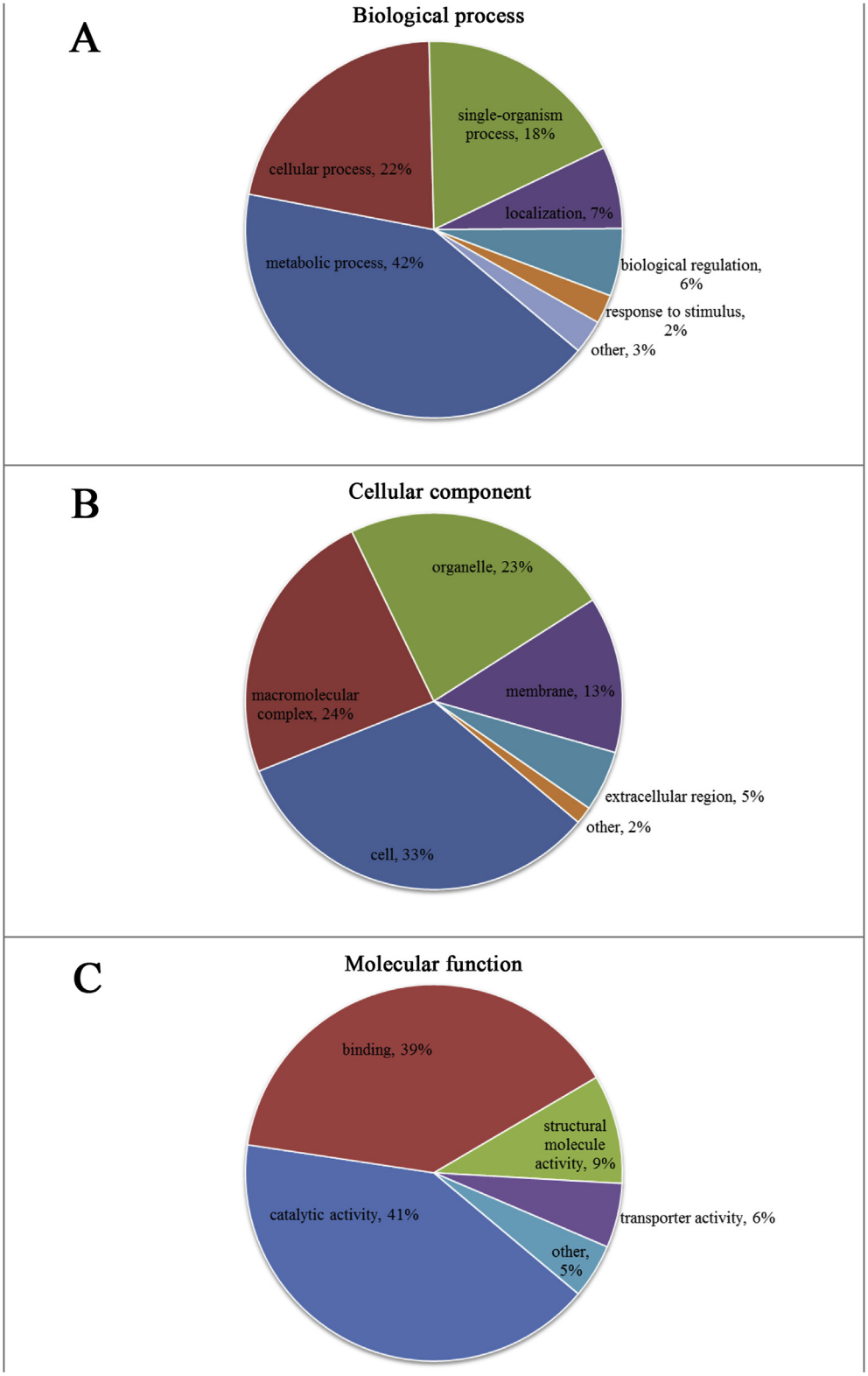

Fig. 2. GO analysis of differential proteins in hepatopancreas. A total of 266 differential proteins were identified by proteomic analysis. Shown above is the classification of these proteins in different categories based on biological processes (A), cellular component (B) and molecular function (C).

further used to determine the potential biomarkers associated with EHP-infected shrimp (Fig. 3B). As shown in Fig. 3C, the validation of this model showed no overfitting phenomenon, which indicated that this model could well describe the samples and could be applied in further data analysis. A heat map (Fig. 4) shows the significantly changed metabolites found between the EHP-infected group (E1-6) and the healthy group (L1-6). 49 distinctly different metabolites ($p < 0.05$) in the EHP-infected groups were identified compared to those of healthy groups (Table 2). Among them, 25 metabolites including spermidine significantly increased in shrimps by EHP infection, while other 24 metabolites such as *N*-Acetyl-D-galactosamine, behenic acid and lignoceric acid significantly decreased in EHP-infected shrimp

Table 1
Representative differential proteins in *L. vannamei* hepatopancreas with a 2-fold change between EHP-challenged and healthy groups.

Protein name	Accession	Score	Coverage [%]	Regulation	Fold change
Immunologic proteins					
alpha2 macroglobulin isoform 2	ACU31810.1	323.31	21.7	↑	2.3
beta-1,3-gluca binding protein	AAW51361.1	65.201	29.1	↑	2.5
C-type lectin	ABU62825.1	202.99	19.1	↑	2.7
lysozyme	AAL23948.1	97.56	24.7	↑	3.1
peritrophin-44-like protein	AIM45534.1	60.644	23	↑	14.0
prophenoloxidase activating enzyme	AFW98991.1	195.13	13.9	↑	2.6
serine proteinase inhibitor	AGL39540.1	323.31	46.8	↑	8.4
cathepsin C	ACG60902.1	20.56	24.6	↓	0.2
cathepsin l	CAA68066.1	323.31	46.6	↓	0.37
C-type lectin	AGV68681.1	45.176	21.4	↓	0.2
ferritin	AAX55641.1	323.31	47.1	↓	0.3
Rab11A	AJC97118.1	145.58	48.1	↓	0.5
Growth associated proteins					
chitin binding-like protein	AFN66647.1	46.909	21.9	↑	2.9
ecdysteroid regulated-like protein	AEX59149.1	26.582	20.9	↑	7.0
farnesoic acid *O*-methyltransferase isoform 1	AAZ22180.1	199.63	38.9	↑	2.8
juvenile hormone esterase-like protein	AKN79605.1	168.3	8.2	↑	4.1
myosin heavy chain type 2	BAM65722.1	323.31	43.2	↑	4.7
myosin light chain	ADD70028.1	174.44	33.8	↑	5.7
chitinase 1C	AHL24866.1	191.04	31.6	↓	0.4
juvenile hormone esterase-like carboxylesterase 1	APO14259.1	239.27	32.6	↓	0.2
steroid reductase	JAC17721.1	26.386	11.2	↓	0.3

compared with healthy groups.

3.5. Pathway analysis

By performing KEGG pathway enrichment analyses, a total of 21 pathways that changed significantly ($p < 0.05$) after EHP infection were identified based on differential proteins (Fig. 5A). Among these pathways,"Metabolism" was the most commonly represented class including several subclasses: "Xenobiotics biodegradation and metabolism", "Metabolism of terpenoids and polyketides", "Metabolism of other amino acids", "Metabolism of cofactors and vitamins", "Energy metabolism", "Carbohydrate metabolism" and "Amino acid metabolism". In addition, some important classes were significantly enriched (e.g., "Organismal systems", "Genetic information processing", "Environmental information processing", "Cellular processes" and "Human diseases"). Most of the pathways we enriched were metabolic pathways, suggesting that EHP infection have affected shrimp metabolism. Interestingly, among the proteomic metabolic pathways, the energy metabolism-related pathways were significantly enriched. It was also known that carbohydrate metabolism allowed cells to access energy, and played an important role in maintaining the energy balance in organisms [29]. Compared with proteins in health shrimps, proteins and pathways related to carbohydrate metabolisms (e.g., "Glycolysis/gluconeogenesis", "Glyoxylate and dicarboxylate metabolism" and "Fructose and mannose metabolism") were significantly enriched in EHP-infected shrimps (Fig. 5A). And, as a pathway of carbohydrate metabolism, "Galactose metabolism" was also significantly affected ($p < 0.05$) when KEGG pathway enrichment for differential metabolites was analyzed (Fig. 5B). In addition to "Galactose metabolism", "Biosynthesis of unsaturated fatty acids" and "ABC transporters" were enriched in metabolome (Fig. 5B). As we known, unsaturated fatty acid could involve in the regulation of energy metabolism [30], and ATP-binding cassette (ABC) transporters could transport many molecules, such as, sugars, amino acids, and lipids to participate in energy metabolism [31]. These features further suggested that the changes of "Biosynthesis of unsaturated fatty acids" and "ABC transporters" pathways indirectly affect the energy balance in EHP-infected shrimps. In a word, these results indicated that there were significant changes in the shrimp energy metabolism at both metabolomic and proteome levels after EHP infection.

3.6. Correlation between gene expressions and protein abundances

To further verify the results of the TMT label-based quantitative analysis and to compare the correlation between protein abundances and gene expressions, qRT-PCR on some selected targets in both the EHP-injection group and healthy group was performed. The mRNA transcription level of twelve proteins was measured, including seven genes of up-regulated proteins (P44L, α2M, PPAE, lysozyme, ERP, FaMeT and Integrin) and five genes of down-regulated proteins (ferritin, Rab11A, CatC, JHEC1 and estradiol 17-beta-dehydrogenase 8 (E_2DH8)) (Fig. 6). As shown in Fig. 6, the qRT-PCR data showed that the transcript abundance of P44L, α2M, PPAE, lysozyme, ERP, FaMeT and Integrin increased by 6.2, 3.1, 0.8, 5.6, 2.4, 0.9, and 0.6-fold, respectively, after EHP-infection, and ferritin, Rab11A, CatC, JHEC1 and E_2DH8 decreased by 1.2, 0.9, 2.6, 0.6, 0.8-fold, respectively. These results indicated that the levels of the gene expressions had similar alteration tendencies with corresponding proteins.

4. Discussion

HPM caused by EHP is a very serious disease of *L. vannamei* in aquaculture. No significant mortality was observed on all occasions of EHP outbreak, but stunted growth was observed in most EHP-positive farms [7,32]. Because the study of HPM has been very limited, little was known about the molecular mechanism of the immune responses and the stunted growth of *L. vannamei* infection by EHP. With advanced analytical techniques, proteomic and metabolomic analyses have become techniques used in frontier research examining the changes or differences in protein regulation and metabolic patterns of tissues [12,33]. This report, to our best knowledge, provides the first proteomes and metabolomes of *L. vannamei* mobilized against an EHP infection, and was a stepping stone on the way to further study of the unique infection mode of this economically important pathogen and other microsporidia in general.

In the study, the proteomes was used to identify 266 differential proteins, among which many immune-related proteins were significantly altered, suggesting that *L. vannamei* innate immune were activated after EHP infection. In addition, significant changes in growth hormone-associated proteins suggested that hormonal balance was disturbed in EHP infected shrimp. In performing KEGG pathway analyses for all differential proteins, EHP infection caused changes in

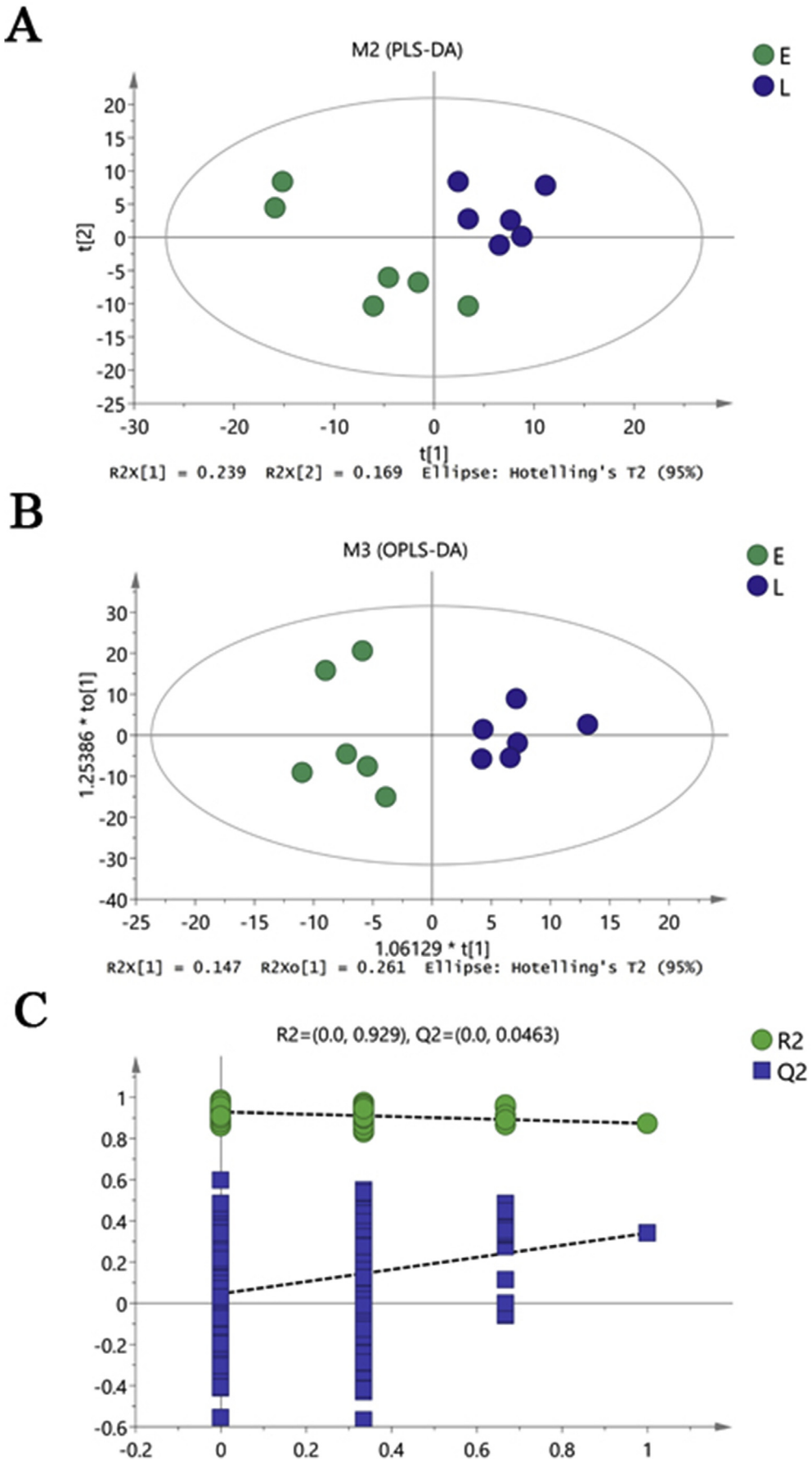

(caption on next page)

Fig. 3. Metabolomic analyses of hepatopancreas samples of stunted growth and healthy shrimp. A, the PLS-DA scores plot based on hepatopancreas metabolic profiles in shrimp. B, the OPLS-DA scores plot based on hepatopancreas metabolic profiles in shrimp. C, the OPLS-DA corresponding validation plot. E, represents metabolic profiles of stunted growth shrimp. L, represents metabolic profiles of healthy shrimp.

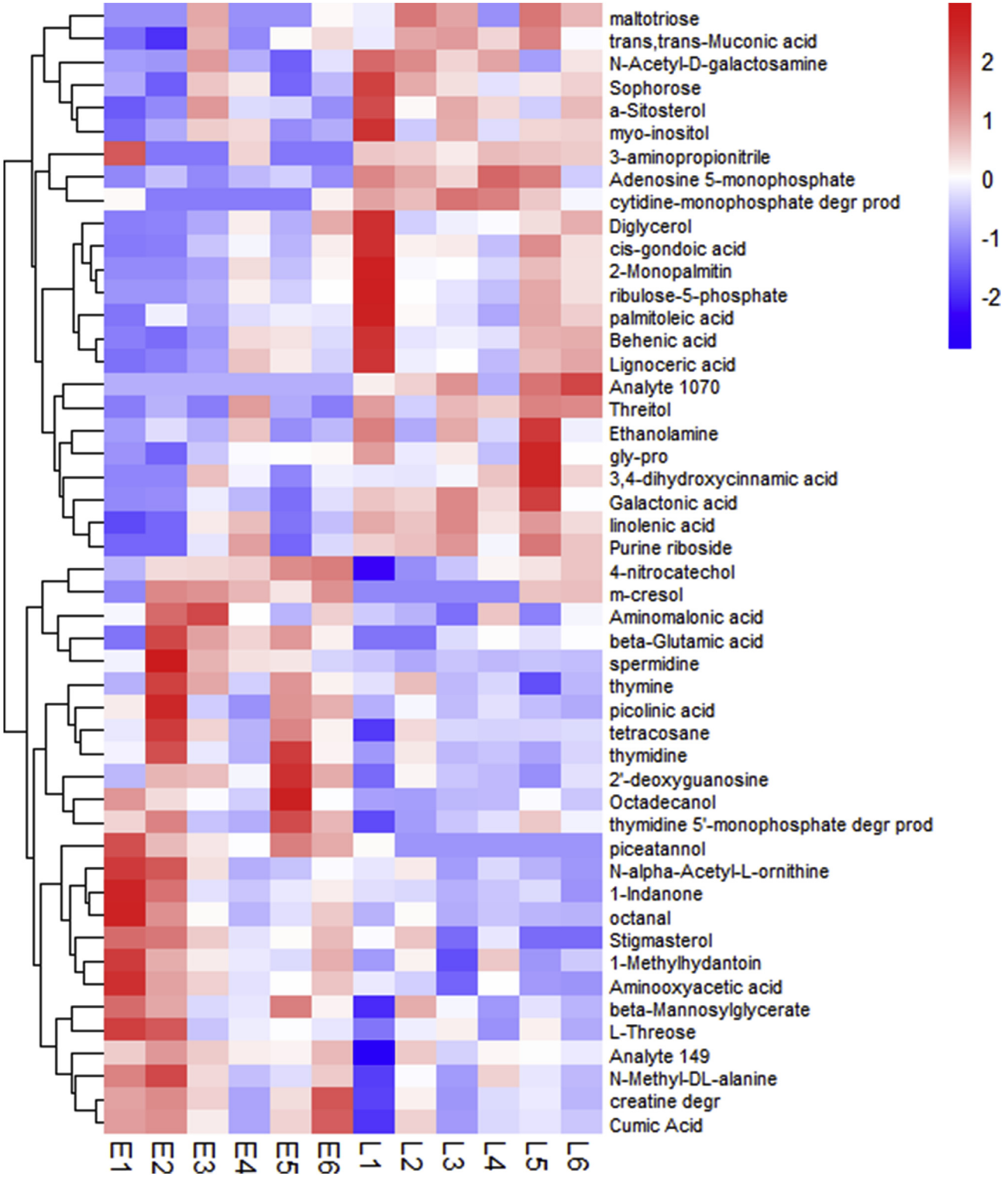

Fig. 4. Heat map representation of the significantly changed metabolites found between EHP-infected group and healthy group. L1-6, health shrimp. E1-6, EHP infected shrimp.

Table 2
Differential metabolites in *L. vannamei* hepatopancreas between EHP-challenged and healthy groups.

Metabolites name	Fold change	Metabolites name	Fold change
piceatannol	10.58	*N*-Acetyl-D-galactosamine	0.78
m-cresol	2.88	trans,trans-Muconic acid	0.77
Stigmasterol	2.71	Sitosterol	0.72
beta-Glutamic acid	2.35	Ethanolamine	0.67
L-Threose	1.94	gly-pro	0.66
thymidine 5′-monophosphate degr prod	1.82	myo-inositol	0.62
Octadecanol	1.75	palmitoleic acid	0.61
thymidine	1.73	linolenic acid	0.60
tetracosane	1.71	Lignoceric acid	0.55
beta-Mannosylglycerate	1.70	Behenic acid	0.52
spermidine	1.70	Sophorose	0.51
picolinic acid	1.68	3-aminopropionitrile	0.44
4-nitrocatechol	1.54	Galactonic acid	0.44
2′-deoxyguanosine	1.43	Diglycerol	0.43
Aminooxyacetic acid	1.40	cis-gondoic acid	0.43
Analyte 149	1.39	2-Monopalmitin	0.39
1-Indanone	1.38	3,4-dihydroxycinnamic acid	0.38
octanal	1.32	Adenosine 5-monophosphate	0.38
thymine	1.24	Purine riboside	0.37
N-Methyl-DL-alanine	1.22	ribulose-5-phosphate	0.32
Aminomalonic acid	1.21	maltotriose	0.31
1-Methylhydantoin	1.19	Threitol	0.27
N-alpha-Acetyl-L-ornithine	1.19	cytidine-monophosphate degr prod	0.21
creatine degr	1.18	Analyte 1070	1.48×10^{-5}
Cumic Acid	1.15		

shrimp metabolism, especially energy metabolism. At the same time, the results of metabolomes further confirmed the change of energy metabolism in shrimp after EHP infection. Therefore, we discuss the immune and metabolic responses in *L. vannamei* against EHP by integrating the large-scale omics data.

4.1. Immune response

Among 148 up-regulated proteins, several proteins (e.g., P44L protein, α2M and PPAE) were related to host immunity. In insects, peritrophic membrane (PM) is believed to constitute a protective barrier for midgut epithelial cells to prevent the intrusion of bacteria, viruses, and other parasites [34–36]. Recently, the study was reported that peritrophin-like gene from *Eriocheir sinensis* was involved in the anti-bacterial innate immunity of crabs [37]. In this study, the translational and transcriptional levels of P44L in *L. vannamei* were all up-regulated after EHP infection. The results suggest that the P44L plays an important role in the process of resistance and clearing up the pathogen. It is well-known that α2M is a broad range proteinase inhibitor and a highly abundant plasma protein that is crucially involved in immune responses [38]. The α2M in *Scylla serrata* response to white spot syndrome virus infection similar with results of this study [39]. Invertebrate prophenoloxidase-activating system (proPO system) is a special and important innate immune defense mechanism that is controlled and regulated by many molecules, such as PPAE [40]. Once pathogens invade the host, the proPO system converts proPO into the active form of phenoloxidase by PPAE [41]. In this data, the transcription and translation of PPAE were up-regulated post-infection. This suggested the proPO system was activated after EHP infection. In addition to the humoral defense responses described above, many immune factors including lysozyme are involved in the cellular defense responses [42]. After the infection of EHP, the lysozyme was significantly up-regulated. And, many lysozymes have chitinase activity to degrade chitin that is a major component of the spore wall. These results suggested that a cellular defense response was triggered. A similar phenomenon was seen in silkworm infection with *Nosema bombycis* [43].

While part of the immune reaction was activated during EHP infection, some immune responses were suppressed. Ferritin is known as a principal extracellular iron storage molecule and plays an important role in the iron-withholding strategy of innate immunity [44]. In the present study, the abundance of ferritin in shrimps was down-regulated after EHP infection. In contrast to current findings, other research on the transcriptional levels and proteome data in *E. sinensis* hemocytes showed that ferritin levels were up-regulated after infection with *S. eriocheiris* [45]. This difference may be the result of different pathogen-host relationships. Rab proteins, a member of the small G protein superfamily, are important regulators of both the rate and directionality of nucleo-cytoplasmic transport [46]. In recent years, more Rab proteins have also been shown to serve a new role in crustacean immunity against bacteria or virus infections [47,48]. In this study, the Rab11A concentration had a prominent decline after EHP infection. Similar with the findings in this research, the Rab mRNA in *Macrobrachium rosenbergii* hemocyte is down-regulated by *S. eriocheiris* infection [12]. And, *Peneaus japonicus* Rab7 protein interacting with white spot syndrome virus (WSSV) VP28 protein is involved in WSSV infection [49]. Cathepsins are considered as an important protease superfamily and are transformed from inactive proenzymes to mature enzymes by the process of proteolytic cleavage. In recent years, more cathepsin proteins have also been found to be involved in crustacean innate immunity [50,51]. In the current research, the concentration of CatC was significantly down-regulated after the challenge by EHP. These results demonstrated that CatC plays an important immune role in *L. vannamei* to EHP challenge.

4.2. Hormone regulation

In addition to inducing an immune reaction of shrimp, growth-related genes of *L. vannamei* were changed after EHP infection. Methyl farnesoate (MF) is a sesquiterpenoid, structurally similar with insect juvenile hormone (JH) and an unepoxidized analogue of JH, deemed the juvenile hormone of crustaceans [52,53]. The pathways for the synthesis and inactivation of sesquiterpenoid hormones are conserved both in insects and crustaceans [54]. FAMeT is the key enzyme in the juvenile hormone biosynthetic pathway, involved in the conversion of farnesoic acid (FA) to MF in the final step of MF synthesis [55]. The results showed that FAMeT protein was strongly up-regulated, suggesting the accelerated synthesis of MF after EHP infection. In addition, the process of MF inactivation was also affected by EHP infection. As specific carboxylesterases, the JHEC1 are involved in the degradation of MF [56,57]. In the study, the JHEC1 was down-regulated after EHP infection. The crustacean grows by periodic molting, which is controlled by the ecdysteroid and molt-inhibiting hormone [58]. ERP is also an important component of crustacean metamorphosis and the ecdysis cascade reaction [59]. Its abundance is suppressed when the ecdysteroid level is high, and expressed when the ecdysteroid is deficient. A high level of ecdysteroid can effectively promote ecdysis and the early gonadal development, but once the concentration of ecdysteroid declines, the time of ecdysis also will be delayed [60]. The results of ERP up-regulation after EHP stimulation suggest that the ecdysteroids were down-regulated to prevent the shrimp from molting. Hormones are essential substrates in organisms that play a key role in the regulation of metabolism, growth, development, and reproduction. So, we suspect that the hormonal balance is disturbed leading to the shrimp's stunted growth after the EHP challenge.

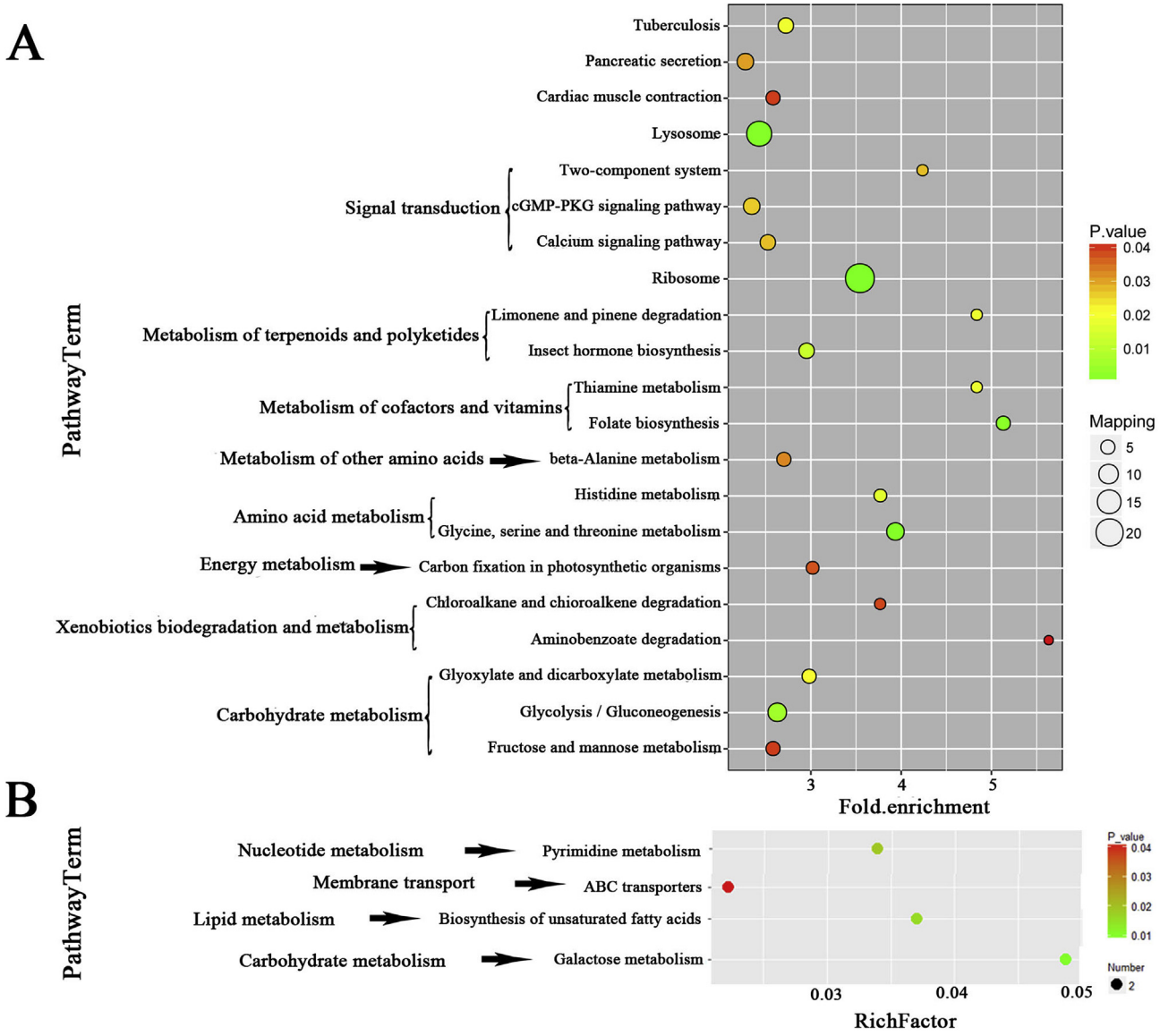

Fig. 5. KEGG pathway enrichment analyses of all differential proteins and metabolites. Twenty-one (A) and four (B) KEGG pathways were obviously enriched in proteomes and metabolomes, respectively (p-value of Fisher's exact test < 0.05).

4.3. Metabolic processes

The intracellular life stages, as well as spores of microsporidia lack any obvious intrinsic means of generating energy. The prevailing view is that their energy is obtained directly from the host [10]. Both proteomic and metabolomic data indicated that metabolic and nutritional pathways were significantly affected after infection with EHP. "Metabolic processes" account for the largest proportion in proteomic GO analysis, and suggested that shrimp metabolism significantly change after EHP infection. Furthermore, subsequent proteomic KEGG pathway analysis confirmed that the differential proteins were mainly concentrated in the metabolic pathways. Among the proteomic metabolic pathways, the energy metabolism pathways were significantly enriched (e.g., "Glycolysis/gluconeogenesis", "Glyoxylate and dicarboxylate metabolism" and "Fructose and mannose metabolism"). In performing KEGG pathway analysis for differentially metabolic biomarkers (e.g., *N*-Acetyl-D-galactosamine, behenic acid and lignoceric acid), "Galactose metabolism" and "Biosynthesis of unsaturated fatty acids" were significantly enriched. The consistency between proteomic KEGG pathways and metabolic KEGG pathways confirmed the disturbance in energy metabolism induced by EHP. Based on these results, EHP could "starve" its hosts through appropriating host resources, resulting in associated changes in shrimp metabolism. This was also similar with previous studies indicating that microsporidian infection was energetically costly [10,61]. ATP-binding cassette (ABC) transporters are integral membrane proteins to translocate solutes across cellular membranes by using cellular energy in all phyla [31]. ABC transporters are involved in diverse cellular processes such as maintenance of nutrient uptake, resistance to xenotoxins and cholesterol and lipid trafficking [62,63]. Many molecules can be transported by ABC transporters, for example, ions, sugars, amino acids, hormones, lipids and xenobiotics [64]. In the study, after EHP infection in the shrimp, metabolic biomarkers of ABC transporters pathway were also significantly changed, indicating the balance of vectorial transport was disturbed. These results suggested that the change in transport ability of carbohydrates and lipids lead directly to the change of the energy metabolism, resulting in an apparent inhibition for the growth and development of shrimp.

In summary, the molecular responses induced by EHP were investigated at protein and metabolite levels in hepatopancreas of *L. vannamei*. The metabolic and proteomic biomarkers suggested that EHP infection could induce an immune response, disturbances in hormone

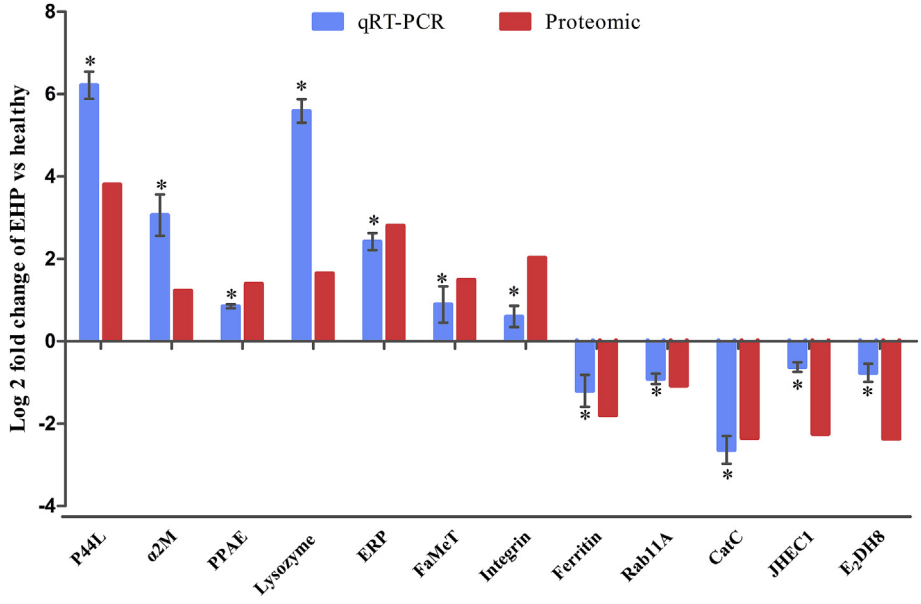

Fig. 6. Verification of the selected differentially expressed genes (DEGs) by qRT-PCR as compared with proteome data. Vertical bars represent mean ± S.E. (n = 30). Asterisks indicate significant differences between EHP-infected shrimp group versus healthy shrimp group ($p < 0.05$).

regulation and energy metabolism in shrimp. More importantly, the changes of hormone regulation and energy metabolism could provide much-needed insight into the underlying mechanisms of stunted growth in shrimp after EHP infection.

Acknowledgments

We thank Professor O. Roger Anderson of Columbia University in the City of New York for editing the manuscript. The current study was supported by grants from the National Natural Sciences Foundation of China (NSFC Nos. 31570176; 31602198; 31870168), Project of the fishery science and technology innovation program (Grant Nos. Y2016-28; Y2017-20; Y2017-34), the Natural Science Foundation of Jiangsu Province (Grant No. BK20151545), Opening Foundation of Jiangsu Provincial Key Construction Laboratory of Probiotics Preparation (JSYSZJ2018006), Nanjing Normal University Excellent Doctoral Dissertation Topic Selection Funding Program (YXXT18-014) and the project funded by the Priority Academic Program Development of Jiangsu Higher Education Institutions (PAPD).

Appendix A. Supplementary data

Supplementary data to this article can be found online at https://doi.org/10.1016/j.fsi.2019.01.051.

References

[1] R.P. Hirt, L.J. Jr, B. Healy, M.W. Dorey, W.F. Doolittle, T.M. Embley, Microsporidia are related to Fungi: evidence from the largest subunit of RNA polymerase II and other proteins, Proc. Natl. Acad. Sci. U.S.A. 96 (2) (1999) 580–585.

[2] G.D. Stentiford, S.W. Feist, D.M. Stone, K.S. Bateman, A.M. Dunn, Microsporidia: diverse, dynamic, and emergent pathogens in aquatic systems, Trends Parasitol. 29 (11) (2013) 567–578.

[3] J. Vávra, J. Lukeš, Microsporidia and 'the art of living together', Adv. Parasitol. 82 (2013) 253–319.

[4] Z. Ma, C. Li, G. Pan, Z. Li, B. Han, J. Xu, X. Lan, J. Chen, D. Yang, Q. Chen, Genome-wide transcriptional response of silkworm (*Bombyx mori*) to infection by the microsporidian *Nosema bombycis*, PLoS One 8 (12) (2013) e84137.

[5] K.V. Rajendran, S. Shivam, P.E. Praveena, J.J.S. Rajan, T.S. Kumar, S. Avunje, V. Jagadeesan, S.P. Babu, A. Pande, A.N. Krishnan, S.V. Alavandi, K.K. Vijayan, Emergence of *Enterocytozoon hepatopenaei* (EHP) in farmed *Penaeus* (*Litopenaeus*) *vannamei* in India, Aquaculture 454 (2016) 272–280.

[6] P. Jaroenlak, P. Sanguanrut, B.A. Williams, G.D. Stentiford, T.W. Flegel, K. Sritunyalucksana, O. Itsathitphaisarn, A Nested PCR Assay to Avoid False Positive Detection of the Microsporidian *Enterocytozoon hepatopenaei* (EHP) in Environmental Samples in Shrimp Farms, PLoS One 11 (11) (2016) e0166320.

[7] S. Santhoshkumar, S. Sivakumar, S. Vimal, S. Abdul Majeed, G. Taju, P. Haribabu, A. Uma, A.S. Sahul Hameed, Biochemical changes and tissue distribution of *Enterocytozoon hepatopenaei* (EHP) in naturally and experimentally EHP-infected whiteleg shrimp, *Litopenaeus vannamei* (Boone, 1931), in India, J. Fish. Dis. 40 (4) (2017) 529–539.

[8] S. Tourtip, S. Wongtripop, G.D. Stentiford, K.S. Bateman, S. Sriurairatana, J. Chavadej, K. Sritunyalucksana, B. Withyachumnarnkul, *Enterocytozoon hepatopenaei* sp. nov. (Microsporida: Enterocytozoonidae), a parasite of the black tiger shrimp *Penaeus monodon* (Decapoda: Penaeidae): fine structure and phylogenetic relationships, J. Invertebr. Pathol. 102 (1) (2009) 21–29.

[9] K.F. Tang, C.R. Pantoja, R.M. Redman, J.E. Han, L.H. Tran, D.V. Lightner, Development of in situ hybridization and PCR assays for the detection of *Enterocytozoon hepatopenaei* (EHP), a microsporidian parasite infecting penaeid shrimp, J. Invertebr. Pathol. 130 (2015) 37–41.

[10] D.W. Boakye, P. Jaroenlak, A. Prachumwat, T.A. Williams, K.S. Bateman, O. Itsathitphaisarn, K. Sritunyalucksana, K.H. Paszkiewicz, K.A. Moore, G.D. Stentiford, Decay of the glycolytic pathway and adaptation to intranuclear parasitism within *Enterocytozoonidae microsporidia*, Environ. Microbiol. 19 (5) (2017) 2077–2089.

[11] H. Schulenburg, C. Boehnisch, N.K. Michiels, How do invertebrates generate a highly specific innate immune response? Mol. Immunol. 44 (13) (2007) 3338–3344.

[12] L. Hou, Y. Xiu, J. Wang, X. Liu, Y. Liu, W. Gu, W. Wang, Q. Meng, iTRAQ-based quantitative proteomic analysis of *Macrobrachium rosenbergii* hemocytes during *Spiroplasma eriocheiris* infection, J. Proteomics. 136 (2016) 112–122.

[13] P.S. Gross, T.C. Bartlett, C.L. Browdy, R.W. Chapman, G.W. Warr, Immune gene discovery by expressed sequence tag analysis of hemocytes and hepatopancreas in the Pacific White Shrimp, *Litopenaeus vannamei*, and the Atlantic White Shrimp, *L. setiferus*, Dev. Comp. Immunol. 25 (7) (2001) 565–577.

[14] P.F. Ji, C.L. Yao, Z.Y. Wang, Immune response and gene expression in shrimp (*Litopenaeus vannamei*) hemocytes and hepatopancreas against some pathogen-associated molecular patterns, Fish Shellfish Immunol. 27 (4) (2009) 563–570.

[15] Z.Y. Zhao, Z.X. Yin, S.P. Weng, H.J. Guan, S.D. Li, K. Xing, S.M. Chan, J.G. He, Profiling of differentially expressed genes in hepatopancreas of white spot syndrome virus-resistant shrimp (*Litopenaeus vannamei*) by suppression subtractive hybridisation, Fish Shellfish Immunol. 22 (5) (2007) 520–534.

[16] E.M. Santos, J.S. Ball, T.D. Williams, H.F. Wu, F. Ortega, R.V. Aerle, I. Katsiadaki, F. Falciani, M.R. Viant, J.K. Chipman, Identifying health impacts of exposure to copper using transcriptomics and metabolomics in a fish model, Environ. Sci. Technol. 44 (2) (2010) 820–826.

[17] Z. Fu, L. Zhang, X. Liu, Y. Zhang, Q. Zhang, X. Li, W. Zheng, L. Sun, J. Tian, Comparative proteomic analysis of the sun- and freeze-dried earthworm *Eisenia fetida* with differentially thrombolytic activities, J. Proteomics. 83 (10) (2013) 1–14.

[18] Z. Li, H. Wu, X. Zhang, X. Li, P. Liao, W. Li, F. Pei, Investigation on the acute biochemical effects of light rare earths on rat serum by NMR-based metabonomic approaches, Front. Chem. China 1 (4) (2006) 443–447.

[19] N.L. Anderson, N.G. Anderson, Proteome and proteomics: new technologies, new concepts, and new words, Electrophoresis 19 (11) (1998) 1853–1861.

[20] S.Y. Khan, M. Ali, F. Kabir, S. Renuse, C.H. Na, T.C. Jr, S.F. Hackett, S.A. Riazuddin, Proteome profiling of developing murine lens through mass spectrometry, Invest. Ophthalmol. Vis. Sci. 59 (1) (2018) 100–107.

[21] V. García-Hernández, C. Sánchez-Bernal, D. Schvartz, J.J. Calvo, J.C. Sanchez, A

tandem mass tag (tmt) proteomic analysis during the early phase of experimental pancreatitis reveals new insights in the disease pathogenesis, J. Proteomics. 181 (2018) 190–200.
[22] J. Feng, J. Zhao, F. Hao, C. Chen, K. Bhakoo, H. Tang, NMR-based metabonomic analyses of the effects of ultrasmall superparamagnetic particles of iron oxide (USPIO) on macrophage metabolism, J. Nanoparticle Res. 13 (5) (2011) 2049–2062.
[23] M.S. Pedras, Q.A. Zheng, Metabolic responses of Thellungiella halophila/salsuginea to biotic and abiotic stresses: metabolite profiles and quantitative analyses, Phytochemistry 71 (5–6) (2010) 581–589.
[24] H. Wu, X. Zhang, X. Li, Z. Li, Y. Wu, F. Pei, Comparison of metabolic profiles from serum from hepatotoxin-treated rats by nuclear-magnetic-resonance-spectroscopy-based metabonomic analysis, Anal. Biochem. 340 (1) (2005) 99–105.
[25] H. Zhang, L. Ding, X. Fang, Z. Shi, Y. Zhang, H. Chen, X. Yan, J. Dai, Biological responses to perfluorododecanoic acid exposure in rat kidneys as determined by integrated proteomic and metabonomic studies, PLoS One 6 (6) (2011) e20862.
[26] Y.P. Liu, G.J. Hang, T.Q. Liu, A.H. Li, D. Xiao, Establishment and application of pcr assay for detection of vibrio spp, Freshw. Fish. 3 (2015) 88–92 (in Chinese).
[27] Z. Ding, J. Chen, J. Lin, X. Zhu, G. Xu, R. Wang, Q. Meng, W. Wang, Development of in situ hybridization and real-time PCR assays for the detection of *Hepatospora eriocheir*, a microsporidian pathogen in the Chinese mitten crab *Eriocheir sinensis*, J. Fish. Dis. 40 (7) (2017) 919–927.
[28] S. Santhoshkumar, S. Sivakumar, S. Vimal, M.S. Abdul, G. Taju, P. Haribabu, A. Uma, A.S. Sahul Hameed, Biochemical changes and tissue distribution of *Enterocytozoon hepatopenaei* (EHP) in naturally and experimentally EHP-infected whiteleg shrimp, *Litopenaeus vannamei* (Boone, 1931), in India, J. Fish. Dis. 40 (4) (2017) 529–539.
[29] M. Dashty, A quick look at biochemistry: carbohydrate metabolism, Clin. Biochem. 46 (15) (2013) 1339–1352.
[30] M.T. Nakamura, B.E. Yudell, J.J. Loor, Regulation of energy metabolism by long-chain fatty acids, Prog. Lipid Res. 53 (1) (2014) 124–144.
[31] P.M. Jones, A.M. George, The ABC transporter structure and mechanism: perspectives on recent research, Cell. Mol. Life. Sci. 61 (6) (2004) 682–699.
[32] A. Tangprasittipap, J. Srisala, S. Chouwdee, M. Somboon, N. Chuchird, C. Limsuwan, T. Srisuvan, T.W. Flegel, K. Sritunyalucksana, The microsporidian *Enterocytozoon hepatopenaei* is not the cause of white feces syndrome in whiteleg shrimp *Penaeus* (*Litopenaeus*) *vannamei*, BMC Vet. Res. 9 (1) (2013) 139.
[33] D.P. Marancik, M.D. Fast, A.C. Camus, Proteomic characterization of the acute-phase response of yellow stingrays *Urobatis jamaicensis* after injection with a *Vibrio anguillarum-ordalii* bacterin, Fish Shellfish Immunol. 34 (5) (2013) 1383–1389.
[34] R.L. Tellam, G. Wijffels, P. Willadsen, Peritrophic matrix proteins, Insect. Biochem. Molec. 29 (2) (1999) 87–101.
[35] D. Hegedus, M. Erlandson, C. Gillott, U. Toprak, New insights into peritrophic matrix synthesis, architecture, and function, Annu. Rev. Entomol. 54 (54) (2009) 285–302.
[36] C.M. Elvin, T. Vuocolo, R.D. Pearson, I.J. East, G.A. Riding, C.H. Eisemann, R.L. Tellam, Characterization of a major peritrophic membrane protein, peritrophin-44, from the larvae of *Lucilia cuprina*, J. Biol. Chem. 271 (15) (1996) 8925–8935.
[37] Y. Huang, F. Ma, W. Wang, Q. Ren, Identification and molecular characterization of a peritrophin-like gene, involved in the antibacterial response in Chinese mitten crab, *Eriocheir sinensis*, Dev. Comp. Immunol. 50 (2) (2015) 129–138.
[38] P.B. Armstrong, R. Melchior, J.P. Quigley, Humoral immunity in long-lived arthropods, J. Insect Physiol. 42 (1) (1996) 53–64.
[39] W. Liu, D. Qian, X. Yan, Proteomic analysis of differentially expressed proteins in hemolymph of *Scylla serrata* response to white spot syndrome virus infection, Aquaculture 314 (1–4) (2011) 53–57.
[40] L. Cerenius, K. Söderhäll, The prophenoloxidase-activating system in invertebrates, Immunol. Rev. 198 (1) (2004) 116–126.
[41] M.W. Johansson, K. Söderhäll, The prophenoloxidase activating systemand associated proteins in invertebrates, Invertebr. Immunol. 15 (1996) 46–66.
[42] S.C. Szumowski, E.R. Troemel, Microsporidia-host interactions, Curr. Opin. Microbiol. 26 (2015) 10–16.
[43] Y.J. Yue, X.D. Tang, L. Xu, W. Yan, Q.L. Li, S.Y. Xiao, X.L. Fu, W. Wang, N. Li, Z.Y. Shen, Early responses of silkworm midgut to microsporidium infection - a Digital Gene Expression analysis, J. Invertebr. Pathol. 124 (2015) 6–14.
[44] S.C. Andrews, P.M. Harrison, S.J. Yewdall, P. Arosio, S. Levi, W. Bottke, M.V. Darl, J.F. Briat, J.P. Laulhère, S. Lobreaux, Structure, function, and evolution of ferritins, J. Inorg. Biochem. 47 (3–4) (1992) 161–174.
[45] Q. Meng, L. Hou, Y. Zhao, X. Huang, Y. Huang, S. Xia, W. Gu, W. Wang, iTRAQ-based proteomic study of the effects of *Spiroplasma eriocheiris* on Chinese mitten crab *Eriocheir sinensis* hemocytes, Fish Shellfish Immunol. 40 (1) (2014) 182–189.
[46] W. Wu, R. Zong, J. Xu, X. Zhang, Antiviral phagocytosis is regulated by a novel Rab-dependent complex in shrimp *Penaeus japonicus*, J. Proteome Res. 7 (1) (2008) 424–431.
[47] L. Wang, L. Li, L. Wang, J. Yang, J. Wang, Z. Zhou, H. Zhang, L. Song, Two Rab GTPases, EsRab-1 and EsRab-3, involved in anti-bacterial response of Chinese mitten crab *Eriocheir sinensis*, Fish Shellfish Immunol. 35 (3) (2013) 1007–1015.
[48] W. Wu, X. Zhang, Characterization of a Rab GTPase up-regulated in the shrimp *Peneaus japonicus* by virus infection, Fish Shellfish Immunol. 23 (2) (2007) 438–445.
[49] K. Sritunyalucksana, W. Wannapapho, F.L. Chu, T.W. Flegel, PmRab7 is a VP28-binding protein involved in white spot syndrome virus infection in shrimp, J. Virol. 80 (21) (2006) 10734–10742.
[50] W.W. Li, L. He, X.K. Jin, H. Jiang, L.L. Chen, Y. Wang, Q. Wang, Molecular cloning, characterization and expression analysis of cathepsin A gene in Chinese mitten crab, *Eriocheir sinensis*, Peptides 32 (3) (2011) 518–525.
[51] W.W. Li, X.K. Jin, L. He, H. Jiang, Y.N. Gong, Y.N. Xie, Q. Wang, Molecular cloning, characterization, expression and activity analysis of cathepsin L in Chinese mitten crab, *Eriocheir sinensis*, Fish Shellfish Immunol. 30 (1) (2010) 1010–1018.
[52] K.C. Holford, K.A. Edwards, W.G. Bendena, S.S. Tobe, Z. Wang, D.W. Borst, Purification and characterization of a mandibular organ protein from the American lobster, *Homarus americanus*: a putative farnesoic acid O-methyltransferase, Insect. Biochem. Molec. 34 (8) (2004) 785–798.
[53] J.H. Hui, S.S. Tobe, S.M. Chan, Characterization of the putative farnesoic acid O-methyltransferase (LvFAMeT) cDNA from white shrimp, *Litopenaeus vannamei*: evidence for its role in molting, Peptides 29 (2) (2008) 252–260.
[54] H. Laufer, D. Borst, F.C. Baker, C.C. Reuter, L.W. Tsai, D.A. Schooley, C. Carrasco, M. Sinkus, Identification of a juvenile hormone-like compound in a crustacean, Science 235 (4785) (1987) 202–205.
[55] Y. Duan, P. Liu, J. Li, Y. Wang, J. Li, P. Chen, A farnesoic acid O-methyltransferase (FAMeT) from *Exopalaemon carinicauda* is responsive to *Vibrio anguillarum* and WSSV challenge, Cell Stress Chaperones 19 (3) (2014) 367–377.
[56] A. Mackert, A.M. do Nascimento, M.M. Bitondi, K. Hartfelder, Z.L. Simões, Identification of a juvenile hormone esterase-like gene in the honey bee, *Apis mellifera* L. - expression analysis and functional assays, Comp. Biochem. Physiol. B Biochem. Mol. Biol. 150 (1) (2008) 33–44.
[57] S.O. Lee, J.M. Jeon, C.W. Oh, Y.M. Kim, C.K. Kang, D.S. Lee, D.L. Mykles, H.W. Kim, Two juvenile hormone esterase-like carboxylesterase cDNAs from a Pandalus shrimp (*Pandalopsis japonica*): cloning, tissue expression, and effects of eyestalk ablation, Comp. Biochem. Physiol. B Biochem. Mol. Biol. 159 (3) (2011) 148–156.
[58] R. Keller, Crustacean neuropeptides: structures, functions and comparative aspects, Experientia 48 (5) (1992) 439–448.
[59] K.J. Lee, T.S. Elton, A.K. Bej, S.A. Watts, R.D. Watson, Molecular cloning of a cDNA encoding putative molt-inhibiting hormone from the blue crab, *Callinectes sapidus*, Biochem. Bioph. Res. Co. 209 (3) (1995) 1126–1131.
[60] C. He, P. Chen, X. Gao, L. Gao, L. Li, Expression and purification of ecdysteroid-regulated protein from Chinese mitten crab *Eriocheir sinensis* in *E. coli*, Mol. Biol. Rep. 40 (12) (2013) 6987–6995.
[61] Z. Ding, J. Pan, H. Huang, G. Jiang, J. Chen, X. Zhu, R. Wang, G. Xu, An integrated metabolic consequence of *Hepatospora eriocheir* infection in the Chinese mitten crab *Eriocheir sinensis*, Fish Shellfish Immunol. 72 (2017) 443–451.
[62] K.D. Bunting, ABC transporters as phenotypic markers and functional regulators of stem cells, Stem Cell. 20 (1) (2002) 11–20.
[63] J. Young, I.B. Holland, ABC transporters: bacterial exporters-revisited five years on, BBA- Biomembranes 1461 (2) (1999) 177–200.
[64] T. Iwaki, Y. Gigahama, K. Takegawa, A survey of all 11 abc transporters in fission yeast: two novel abc transporters are required for red pigment accumulation in a *Schizosaccharomyces pombe* adenine biosynthetic mutant, Microbiology 152 (Pt 8) (2006) 2309–2321.